

On the Capacity of Opportunistic Time-Sharing Downlink with a Reconfigurable Intelligent Surface

Donatella Darsena, *Senior Member, IEEE* and Francesco Verde, *Senior Member, IEEE*

Abstract—We provide accurate approximations of the sum-rate capacity of an opportunistic time-sharing downlink, when a reconfigurable intelligent surface (RIS) assists the transmission from a single-antenna base station (BS) to single-antenna user equipments (UEs). We consider the fading effects of both the direct (i.e., BS-to-UEs) and reflection (i.e., BS-to-RIS-to-UEs) links, by developing two approximations: the former one is based on hardening of the reflection channel for large values of the number of meta-atoms; the latter one relies on the distribution of the sum of Nakagami variates and does not require channel hardening. Our derivations show the dependence of the sum-rate capacity as a function of both the number of users and the number of meta-atoms, as well as to establish a comparison with a downlink without an RIS. Numerical results corroborate the accuracy and validity of the mathematical analysis.

Index Terms—Downlink transmission, opportunistic time sharing, reconfigurable intelligent surface (RIS).

I. INTRODUCTION

IN this letter, we consider a downlink channel in which a *reconfigurable intelligent surface (RIS)* is employed to assist the transmission from a single-antenna transmitter towards $K \gg 1$ single-antenna user equipments (UEs). An RIS is a metasurface composed of sub-wavelength meta-atoms, whose reflection coefficients can be designed via software in order to suitably manipulate the impinging signal [1]. Relying on the feasibility of engineering the meta-atoms, the wireless propagation environment might be programmed by optimizing on-the-fly the reflecting properties of an RIS to achieve different network-wide aims [2].

When the base station (BS) can track the composite channels of the UEs, *opportunistic time sharing* is a simple and effective transmission technique, which allows the BS to use time-division multiplexing and transmit to the best user. Such a scheduling strategy has been shown to achieve the sum-rate capacity (maximum throughput) of the single-antenna downlink channel [3]. A relevant question to ask is the following: *How large of a performance boost does RIS-aided opportunistic time-sharing downlink provide over its*

conventional (i.e., without RIS) counterpart in terms of sum-rate? The scaling law of the sum-rate capacity of a Gaussian downlink with many users K using opportunistic time sharing has been deeply studied without an RIS [4]. A similar study for an RIS-aided downlink with a large number of users K and meta-atoms Q has not been carried out yet.

We focus on the sum-rate capacity achievable using opportunistic time sharing in RIS-aided downlinks. We develop an approximation of the sum-rate capacity by invoking hardening of the reflection channel in the large Q limit, which allows to readily unveil the scaling laws as a function of K and Q . Furthermore, we provide a very accurate approximation of the sum-rate capacity without invoking channel hardening, which is based on the sum of Nakagami variates. We also investigate the interplay between the gain offered by the RIS and the selection diversity among the UEs.

II. SIGNAL MODEL AND PRELIMINARIES

As in [5], the downlink transmission among the BS and K UEs is assisted by a digitally programmable RIS working in reflection mode, which is made of $Q = Q_x \times Q_y$ meta-atoms that can be independently and dynamically controlled by digital logic devices [1]. The meta-atoms are positioned along a rectangular grid having Q_x and Q_y elements on the x and y axes, respectively, with constant inter-element spacing d_{RIS} . The channel between the BS and the RIS is assumed to be characterized by a dominant line-of-sight component, which is modeled as $\mathbf{g} = \sigma_g \mathbf{a}_{\text{RIS}}$, with pathloss σ_g^2 and signature

$$\mathbf{a}_{\text{RIS}} \triangleq \left[1, e^{j \frac{2\pi}{\lambda_0} d_{\text{RIS}} u_x}, \dots, e^{j \frac{2\pi}{\lambda_0} (Q_x - 1) d_{\text{RIS}} u_x} \right]^T \otimes \left[1, e^{j \frac{2\pi}{\lambda_0} d_{\text{RIS}} u_y}, \dots, e^{j \frac{2\pi}{\lambda_0} (Q_y - 1) d_{\text{RIS}} u_y} \right]^T \in \mathbb{C}^Q$$

where $\lambda_0 = c/f_0$ is the wavelength, c is the speed of the light in the medium, $\theta_{\text{RIS}} \in [0, 2\pi)$ and $\phi_{\text{RIS}} \in [-\pi/2, \pi/2)$ identify the azimuth and elevation angles, respectively, the corresponding directional cosines are $u_x \triangleq \sin \theta_{\text{RIS}} \cos \phi_{\text{RIS}}$ and $u_y \triangleq \sin \theta_{\text{RIS}} \sin \phi_{\text{RIS}}$, and \otimes is the Kronecker product.

All the other relevant links are modeled as narrowband frequency-flat channels. Specifically, for $k \in \{1, 2, \dots, K\}$, $h_k \sim \mathcal{CN}(0, \sigma_{h_k}^2)$ models the low-pass equivalent channel response from the BS to UE k , whereas $\mathbf{f}_k \sim \mathcal{CN}(\mathbf{0}_Q, \sigma_{f_k}^2 \mathbf{I}_Q)$ represents the low-pass equivalent channel response from the RIS to the k -th UE. The parameters $\sigma_{h_k}^2$ and $\sigma_{f_k}^2$ are the large-scale geometric path losses of the links seen by the k -th UE with respect to the BS and the RIS, respectively.

We customarily assume that each UE uses standard timing synchronization with respect to its direct link. After matched

Manuscript received August 26, 2023; accepted October 4, 2023. Date of publication xx yy 2023; date of current version xx yy 2023. This work was partially supported by the European Union under the Italian National Recovery and Resilience Plan (NRRP) of NextGenerationEU, partnership on “Telecommunications of the Future” (PE00000001 - program “RESTART”). The associate editor coordinating the review of this article and approving it for publication was Dr. Gang Yang. (*Corresponding author: Francesco Verde.*)

F. Verde and D. Darsena are with the Department of Electrical Engineering and Information Technology, University Federico II, Naples I-80125, Italy [e-mail: (f.verde, darsena)@unina.it]. The Authors are also with National Inter-University Consortium for Telecommunications (CNIT).

Digital Object Identifier xxxxxxxxxxxxxxxxxxxx.

filtering and sampling at the baud rate, the discrete-time baseband signal received at the k -th user reads as

$$r_k = c_k^* \left(\sum_{u=1}^K \sqrt{\mathcal{P}_u} s_u \right) + v_k$$

where the *overall* channel gain seen by the k -th UE is $c_k \triangleq h_k + \mathbf{g}^H \mathbf{\Gamma}^* \mathbf{f}_k \in \mathbb{C}$, for $k \in \{1, 2, \dots, K\}$, with the q -th diagonal entry of $\mathbf{\Gamma} \triangleq \text{diag}(\gamma_1, \gamma_2, \dots, \gamma_Q)$ representing the reflection coefficient of the q -th meta-atom, s_u being the information-bearing symbol intended for the u -th user with corresponding transmit power \mathcal{P}_u , and $v_k \sim \mathcal{CN}(0, 1)$ is the noise sample at the output of the matched filter, with v_{k_1} statistically independent of v_{k_2} , for $k_1 \neq k_2$. The transmitted symbols s_1, s_2, \dots, s_K are independent and identically distributed (i.i.d.) complex circular zero-mean unit-variance random variables (RVs). The couple (h_k, \mathbf{f}_k) is independent of both v_k and s_k , $\forall k \in \{1, 2, \dots, K\}$.

The *sum-rate capacity* (in bits/s/Hz) is defined as follows

$$C_{\text{sum}} = \max_{\substack{\mathcal{P}_1, \mathcal{P}_2, \dots, \mathcal{P}_K \\ \gamma_1, \gamma_2, \dots, \gamma_Q}} \sum_{k=1}^K \log_2 \left(1 + \frac{\mathcal{P}_k |c_k|^2}{|c_k|^2 \sum_{u \neq k} \mathcal{P}_u + 1} \right)$$

subject to the *transmit power constraint* $\sum_{k=1}^K \mathcal{P}_k \leq \mathcal{P}_{\text{TX}}$, with $\mathcal{P}_{\text{TX}} > 0$ being the (fixed) maximum allowed transmit power, and the *global passivity constraint* $\|\gamma\|^2 \leq Q$ at the RIS [6], with $\gamma \triangleq [\gamma_1, \gamma_2, \dots, \gamma_Q]^H \in \mathbb{C}^Q$. For a lossless RIS, the latter constraint yields $\|\gamma\|^2 = Q$.¹

Given the reflection vector γ , the sum-rate capacity is equal to the largest single-user capacity in the system [3], that is, the resource allocation policy is the opportunistic time-sharing strategy: $\mathcal{P}_k = \mathcal{P}_{\text{TX}}$ if $k = k_{\text{max}}$, $\mathcal{P}_k = 0$ otherwise, with $k_{\text{max}} \triangleq \arg \max_{k \in \{1, 2, \dots, K\}} |c_k|^2$. Recalling the expression of c_k , the corresponding sum-rate capacity boils down to

$$C_{\text{sum}} = \log_2 (1 + \mathcal{P}_{\text{TX}} \alpha_{\text{opt}}) \quad (1)$$

with

$$\alpha_{\text{opt}} \triangleq \max_{\substack{k \in \{1, 2, \dots, K\} \\ \gamma \in \mathbb{C}^Q: \|\gamma\|^2 = Q}} |h_k|^2 + 2 \Re \{ \beta_k^H \gamma \} + \gamma^H \mathbf{B}_k \gamma \quad (2)$$

where $\beta_k \triangleq h_k \text{diag}(\mathbf{f}_k^*) \mathbf{g} \in \mathbb{C}^Q$ and we have defined the Hermitian matrix $\mathbf{B}_k \triangleq \text{diag}(\mathbf{f}_k^*) \mathbf{g} \mathbf{g}^H \text{diag}(\mathbf{f}_k) \in \mathbb{C}^{Q \times Q}$. Closed-form solution of (2) is provided by Lemma 2.1.

Lemma 2.1: Under the constraint $\|\gamma\|^2 = Q$, the cost function in (2) can be upper bounded for each k as follows

$$|h_k|^2 + 2 \Re \{ \beta_k^H \gamma \} + \gamma^H \mathbf{B}_k \gamma \leq \left(|h_k| + \sqrt{Q} \|\text{diag}(\mathbf{f}_k^*) \mathbf{g}\| \right)^2$$

where the equality holds if and only if

$$\gamma = \sqrt{Q} \frac{h_k \text{diag}(\mathbf{f}_k^*) \mathbf{g}}{|h_k| \|\text{diag}(\mathbf{f}_k^*) \mathbf{g}\|}. \quad (3)$$

Proof: The proof comes from: (a) $\Re\{x\} \leq |x| \forall x \in \mathbb{C}$; (b) the Cauchy-Schwarz inequality $|\beta_k^H \gamma| \leq \|\beta_k\| \|\gamma\|$; (c)

¹Another option for a lossless RIS consists of imposing the Q *local passivity constraints* $|\gamma_q| = 1, \forall q \in \{1, 2, \dots, Q\}$ [5]. However, in this case, optimization of the reflection response is a non-convex NP-hard problem. The best known methods that develop a solution for this problem are iterative and do not provide a closed-form solution.

the Rayleigh-Ritz theorem and observing that the maximum eigenvalue of the rank-one matrix \mathbf{B}_k is $\|\text{diag}(\mathbf{f}_k^*) \mathbf{g}\|^2$.

Physically, solution (3) implies that the RIS may introduce local power amplifications (i.e., $|\gamma_q| > 1$) or local power losses (i.e., $|\gamma_q| < 1$) for some meta-atoms, while ensuring that the total reradiated power by the lossless RIS is equal to the total incident power (see [6] for implementation details).

III. THEORETICAL PERFORMANCE ANALYSIS

By applying channel coding across channel coherence intervals (i.e., over an “ergodic” interval of channel variation with time), the *average* sum-rate capacity [3] is given by

$$\bar{C}_{\text{sum}} \triangleq \mathbb{E}[C_{\text{sum}}] = \int_0^{+\infty} \log_2 (1 + \mathcal{P}_{\text{TX}} \alpha) f_{\alpha_{\text{opt}}}(\alpha) d\alpha \quad (4)$$

where $f_{\alpha_{\text{opt}}}(\alpha)$ is the probability density function (pdf) of the RV α_{opt} , which, by virtue of Lemma 2.1, can be explicitly written as $\alpha_{\text{opt}} = \max_{k \in \{1, 2, \dots, K\}} (|h_k| + \sqrt{Q} \|\text{diag}(\mathbf{f}_k^*) \mathbf{g}\|)^2$. Under the opportunistic time-sharing strategy, there is just one user transmitting at any time and, thus, we can resort to the encoding and decoding procedures for the code designed for a point-to-point channel [3].

We consider the case in which the users approximately experience the same large-scale geometric path loss, i.e., the parameters $\sigma_{h_k}^2$ and $\sigma_{f_k}^2$ do not depend on k , i.e., $\sigma_{h_k}^2 \equiv \sigma_h^2$ and $\sigma_{f_k}^2 \equiv \sigma_f^2, \forall k \in \{1, 2, \dots, K\}$, which will be referred to as the case of *homogeneous* users.² In this case, the RV α_{opt} is the maximum of K i.i.d. RVs and its pdf is computed as

$$f_{\alpha_{\text{opt}}}(\alpha) = K f_{X_k}(\alpha) [F_{X_k}(\alpha)]^{K-1} \quad (5)$$

where $f_{X_k}(\alpha)$ and $F_{X_k}(\alpha)$ denote the pdf and the cumulative distribution function (cdf) of the RV $X_k \triangleq Z_k^2$, with $Z_k \triangleq Z_k^{(1)} + Z_k^{(2)}$, $Z_k^{(1)} \triangleq |h_k|$, and $Z_k^{(2)} \triangleq \sigma_g \sqrt{Q} \|\mathbf{f}_k\|$. The distributions of $Z_k^{(1)}$ and $Z_k^{(2)}$ are discussed in Appendix A.

Trying to work with (5) for evaluating (4) is numerically difficult even for small values of K . Hence, we apply extreme value theory [7] to calculate the distribution of α_{opt} when K is sufficiently large. Relying on the limit laws for maxima [7], provided that the cdf of X_k is a von Mises function,³ as $K \rightarrow \infty$, the RV α_{opt} converges in distribution [8] to the Gumbel distribution $\lim_{K \rightarrow \infty} F_{\alpha_{\text{opt}}}(\alpha) = e^{-e^{-\frac{\alpha - b_K}{a_K}}}$, where $F_{\alpha_{\text{opt}}}(\alpha)$ is the cdf of α_{opt} , whereas

$$b_K \triangleq F_{X_k}^{-1} \left(1 - \frac{1}{K} \right) \text{ and } a_K \triangleq \frac{1}{K f_{X_k}(b_K)}. \quad (6)$$

Replacing $f_{\alpha_{\text{opt}}}(\alpha)$ with the Gumbel pdf, eq. (4) reads as

$$\bar{C}_{\text{sum}} \asymp \frac{1}{a_K} \int_0^{+\infty} \log_2 (1 + \mathcal{P}_{\text{TX}} \alpha) e^{-\frac{\alpha - b_K}{a_K}} e^{-e^{-\frac{\alpha - b_K}{a_K}}} d\alpha \quad (7)$$

²From a physical viewpoint, this happens when the users form a *cluster*, wherein the distances between the different UEs are negligible with respect to the distance between the transmitter and the RIS.

³It fulfills [9] $\lim_{\alpha \rightarrow +\infty} \left[\frac{1 - F_{X_k}(\alpha)}{f_{X_k}(\alpha)} \right] \frac{d}{d\alpha} f_{X_k}(\alpha) = -1$.

with $x \asymp y$ indicating that $\lim_{K \rightarrow +\infty} x/y = 1$.⁴

The pdf or cdf of X_k must be derived to evaluate \bar{c}_{sum} by using either (4)-(5) or (7). To approximate the distribution of X_k , we distinguish two cases: in Subsection III-A, we assume that the reflection channel from the RIS to each UE hardens for sufficiently large values of Q ; in Subsection III-B, we derive a more general approximation that does not require hardening of the reflection channel. In Subsection III-C, we derive the average *receive* signal-to-noise ratio (SNR) of the user selected for scheduling, which allows us to discuss the impact of the parameters K and Q on system performance.

A. Approximation 1: Hardening of the reflection channel

The k -th reflection channel hardens [10] if $Z_k^{(2)}/\mathbb{E}[Z_k^{(2)}]$ converges in probability to 1, as $Q \rightarrow +\infty$, for each $k \in \{1, 2, \dots, K\}$. Based on the Markov inequality [13], a sufficient condition for the hardening of $Z_k^{(2)}$ is $\text{VAR}[Z_k^{(2)}]/\mathbb{E}^2[Z_k^{(2)}] \rightarrow 0$, as $Q \rightarrow +\infty$. By virtue of (14) and (15), one gets $\text{VAR}[Z_k^{(2)}]/\mathbb{E}^2[Z_k^{(2)}] \approx 1/(4Q)$ for very large Q . Therefore, as $Q \rightarrow +\infty$, the pdf of $Z_k^{(2)}$ can be approximated by the following Dirac delta distribution $f_{Z_k^{(2)}}(\alpha) \approx \delta(\alpha - \mathbb{E}[Z_k^{(2)}])$, with the mean of $Z_k^{(2)}$ given by (14). Accordingly, relying on the results of the transformations of RVs [11], the pdf of X_k is approximated by

$$f_{X_k}(\alpha) \approx \frac{\sqrt{\alpha - \mathbb{E}[Z_k^{(2)}]}}{\sigma_h^2 \sqrt{\alpha}} e^{-\frac{(\sqrt{\alpha - \mathbb{E}[Z_k^{(2)}]})^2}{\sigma_h^2}}, \quad \text{for } \alpha > \mathbb{E}[Z_k^{(2)}].$$

After algebraic manipulations, the cdf of X_k is correspondingly approximated:

$$F_{X_k}(\alpha) \approx 1 - e^{-\frac{(\sqrt{\alpha - \mathbb{E}[Z_k^{(2)}]})^2}{\sigma_h^2}}, \quad \text{for } \alpha > \mathbb{E}[Z_k^{(2)}]. \quad (8)$$

For any value of K , the above distributions can be substituted in (5) in order to obtain an approximation of the pdf of α_{opt} , which is involved in the calculus of the average sum-rate capacity (4). On the other hand, since the distribution (8) is a von Mises function, one can resort to (7) for sufficiently large values of K , where (6) ends up to

$$b_K \approx \left[\sigma_f \sigma_g Q + \sigma_h \sqrt{\ln(K)} \right]^2 \quad \text{and} \quad a_K \approx \sigma_h^2 + \frac{\sigma_f \sigma_g \sigma_h Q}{\sqrt{\ln(K)}}. \quad (9)$$

B. Approximation 2: Sum of Nakagami variates

The RV Z_k is the sum of the two independent and non-identically distributed (i.n.i.d.) Nakagami RVs $Z_k^{(1)}$ and $Z_k^{(2)}$. Therefore, the pdf of Z_k is the convolution of the pdfs of $Z_k^{(1)}$ and $Z_k^{(2)}$, which does not admit a closed-form expression. Following [12], we propose to approximate the pdf $f_{Z_k}(\alpha)$ of Z_k by the pdf $f_{\hat{Z}_k}(\alpha)$ of the RV $\hat{Z}_k \triangleq \sqrt{[\hat{Z}_k^{(1)}]^2 + [\hat{Z}_k^{(2)}]^2}$, where $\hat{Z}_k^{(1)}$ and $\hat{Z}_k^{(2)}$ are i.i.d. Nakagami RVs with shape parameter \hat{m} and scale parameter $\hat{\Omega}$, which are determined

⁴By using the Maclaurin series of the exponential function, the integral (7) can be rewritten as an absolutely convergent series, which can be approximately evaluated by using a finite number of terms [9, Appendix C].

such that $f_{\hat{Z}_k}(\alpha)$ be an accurate approximation of $f_{Z_k}(\alpha)$. The choice of \hat{m} and $\hat{\Omega}$ is discussed in Appendix B.

At this point, we would like to point out that the main advantage of using $f_{\hat{Z}_k}(\alpha)$ *in lieu* of $f_{Z_k}(\alpha)$ stems from the fact that the square of \hat{Z}_k is the sum of two i.i.d. gamma RVs [13]. Indeed, the square of a Nakagami RV with shape parameter \hat{m} and scale parameter $\hat{\Omega}$ turns out to be a gamma RV with shape parameter \hat{m} and scale parameter $\hat{\Omega}/\hat{m}$. Moreover, the sum of the two i.i.d. gamma RVs $[\hat{Z}_k^{(1)}]^2$ and $[\hat{Z}_k^{(2)}]^2$ is a gamma RV, too, with shape parameter $2\hat{m}$ and scale parameter $\hat{\Omega}/\hat{m}$. Thus, we can conclude that the pdf of the RV $\hat{X}_k \triangleq \hat{Z}_k^2$ is given by (see, e.g., [13])

$$f_{\hat{X}_k}(\alpha) = \left(\frac{\hat{m}}{\hat{\Omega}} \right)^{2\hat{m}} \frac{\alpha^{2\hat{m}-1}}{\Gamma(2\hat{m})} e^{-\frac{\hat{m}}{\hat{\Omega}}\alpha}, \quad \text{for } \alpha > 0 \quad (10)$$

whose cdf reads as $F_{\hat{X}_k}(\alpha) = P\left(\frac{\hat{m}\alpha}{\hat{\Omega}}, 2\hat{m}\right)$,⁵ where $P(x, a) \triangleq \frac{1}{\Gamma(a)} \int_0^x t^{a-1} e^{-t} dt$ is the (regularized) lower incomplete gamma function and $\Gamma(a)$ is defined in Appendix A.

According to (6), the constant b_K is the solution of $P\left(\frac{\hat{m}b_K}{\hat{\Omega}}, 2\hat{m}\right) = 1 - \frac{1}{K}$, which is given by

$$b_K \approx \frac{\hat{\Omega}}{\hat{m}} P^{-1}\left(1 - \frac{1}{K}, 2\hat{m}\right) \quad (11)$$

where $P^{-1}(y, a)$ is the inverse of the lower incomplete gamma function for $y \in [0, 1]$, i.e., $P^{-1}(P(x, a), a) = x$. Substituting (11) in (6) and replacing $f_{X_k}(b_K)$ with $f_{\hat{X}_k}(b_K)$, one has

$$a_K \approx \frac{\hat{\Omega}}{\hat{m}} \frac{\Gamma(2\hat{m})}{K \left[P^{-1}\left(1 - \frac{1}{K}, 2\hat{m}\right) \right]^{2\hat{m}-1} e^{-P^{-1}\left(1 - \frac{1}{K}, 2\hat{m}\right)}}. \quad (12)$$

C. Average receive SNR

The asymptotic Gumbel distribution allows one to statistically characterize the receive SNR of the user selected for scheduling, which is defined as $\rho_{\text{sum}} \triangleq \mathcal{P}_{\text{TX}} \alpha_{\text{opt}}$. The average receive SNR $\bar{\rho}_{\text{sum}} \triangleq \mathbb{E}[\rho_{\text{sum}}] = \mathcal{P}_{\text{TX}} \mathbb{E}[\alpha_{\text{opt}}]$ can be derived from the mean of the Gumbel distribution, thus yielding

$$\bar{\rho}_{\text{sum}} = \mathcal{P}_{\text{TX}} (b_K + C a_K) \quad (13)$$

with $C \approx 0.5772$ being the Euler-Mascheroni constant.

In a downlink *without* an RIS, the RV $X_k = [Z_k^{(1)}]^2 = |h_k|^2$ is exponentially distributed with mean σ_h^2 . In this case, it follows from (6) that $b_K = \sigma_h^2 \ln(K)$ and $a_K = \sigma_h^2$. From (13), the average receive SNR in an RIS-unaided opportunistic time-sharing downlink is

$$\bar{\rho}_{\text{sum}}^{\text{w/o RIS}} = \mathcal{P}_{\text{TX}} \sigma_h^2 [C + \ln(K)] \Rightarrow \lim_{K \rightarrow +\infty} \frac{\bar{\rho}_{\text{sum}}^{\text{w/o RIS}}}{\ln(K)} = \mathcal{P}_{\text{TX}} \sigma_h^2$$

which benefits by a factor of $\ln(K)$ asymptotically for large K (so-called *multiuser diversity effect*), and $\bar{c}_{\text{sum}}^{\text{w/o RIS}}$ increases double logarithmically in K [4].

⁵It can be verified that $F_{\hat{X}_k}(\alpha)$ is a von Mises function, too.

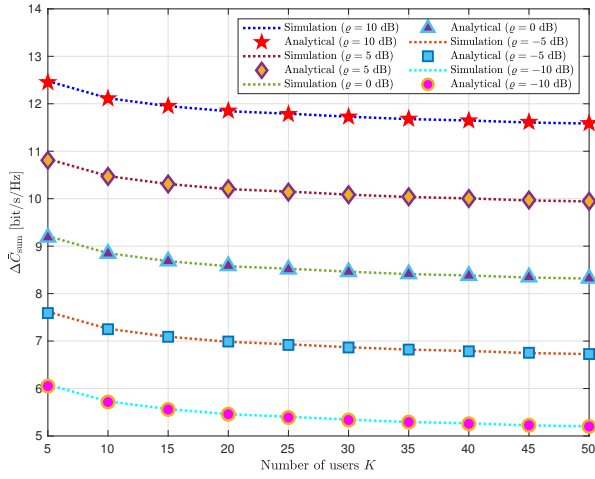


Fig. 1. $\Delta\bar{C}_{\text{sum}}$ versus K (Approximation 2 for the analytical curves).

For a RIS-aided downlink, let us first consider the case when $K \rightarrow +\infty$ and the reflection channel hardens. In this situation, using (9), the average receive SNR in (13) is approximated as

$$\bar{\rho}_{\text{sum}} \approx \bar{\rho}_{\text{sum}}^{\text{w/o RIS}} + \mathcal{P}_{\text{TX}} \left[\sigma_f^2 \sigma_g^2 Q^2 + \sigma_f \sigma_g \sigma_h \frac{2 \ln(K) + C}{\sqrt{\ln(K)}} Q \right]$$

which shows that, compared to the RIS-unaided downlink, the SNR gain provided by the presence of the RIS depends on the relationship between K and Q . Indeed, if Q approaches infinity at the same rate as K , i.e., $Q = \chi K$, where $\chi \neq 0$ is a constant independent of K , it results that $\lim_{K, Q \rightarrow +\infty} \bar{\rho}_{\text{sum}}/Q^2 = \mathcal{P}_{\text{TX}} \sigma_f^2 \sigma_g^2$, i.e., the average receive SNR scales like Q^2 as K and Q grow to infinity. In this case, the downlink performance is dominated by the reflection channel and the reflection process of the RIS becomes predominant with respect to multiuser diversity effects. On the other hand, if Q approaches $+\infty$ as $Q = \chi \sqrt{\ln(K)}$, one has $\lim_{K, Q \rightarrow +\infty} \bar{\rho}_{\text{sum}}/\ln(K) = \mathcal{P}_{\text{TX}} [(\sigma_f \sigma_g \chi + \sigma_h)^2 + C \sigma_f \sigma_g \sigma_h \chi]$. In this case, the sum-rate capacity also depends on the direct channel and the effect of the RIS becomes negligible when $\sigma_f \sigma_g \chi \ll \sigma_h$, thus approaching the performance of the RIS-unaided downlink.

When K grows to infinity and hardening of the reflection channel does not hold, we resort to (10) for approximating the distribution of X_k . In this case, the average receive SNR can be obtained by substituting (11) and (12) in (13), whose dependence on K and Q will be shown numerically in the forthcoming Section IV.

IV. NUMERICAL PERFORMANCE ANALYSIS

We consider a 2-D Cartesian system, wherein the BS and the RIS are located at $(0, 0)$ and $(10, 0)$ (in meters), respectively, whereas the users form a circular cluster centered in $(40, -10)$ (in meters). The inter-element spacing is fixed to $d_{\text{RIS}} = \lambda_0/4$, whereas the azimuth and elevation angles at the RIS are uniformly distributed in $[0, 2\pi)$ and $[-\pi/2, \pi/2)$, respectively. All the other channel links are independently generated by assuming a carrier frequency $f_0 = 25$ GHz, with variance $\sigma_\alpha^2 = G_\alpha d_\alpha^{-\eta} \lambda_0^2 / (4\pi)^2$, for $\alpha \in \{g, h\}$, where $G_\alpha = 25$ dBi for the RIS and $G_\alpha = 5$ dBi for the UEs, while d_α represents

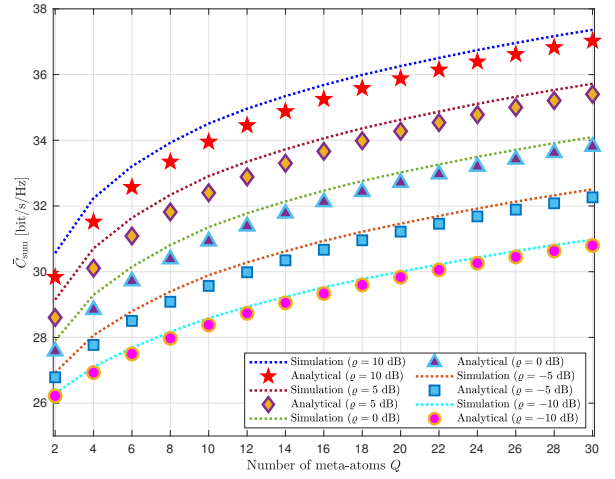


Fig. 2. \bar{C}_{sum} versus Q ($K = 10$, Approximation 1 for the analytical curves).

the distance of the link and $\eta = 1.6$ is the path loss exponent. The variance σ_f^2 of the channel link between the RIS and the UEs is derived from the ratio $\rho \triangleq (\sigma_f^2 \sigma_g^2) / \sigma_h^2$, which assumes the values in $\{0, \pm 5, \pm 10\}$ dB. The effective isotropic radiated power of the BS is set to 33 dBm and the noise power at the UEs is equal to -100 dBm.

In Fig. 1, we report the difference $\Delta\bar{C}_{\text{sum}} \triangleq \bar{C}_{\text{sum}} - \bar{C}_{\text{sum}}^{\text{w/o RIS}}$ between the average sum-rate capacity of the RIS-aided and RIS-unaided downlinks, as a function of the number of users K for different values of ρ . The rates \bar{C}_{sum} and $\bar{C}_{\text{sum}}^{\text{w/o RIS}}$ are numerically obtained by averaging (1) over 1000 independent Monte Carlo runs, by setting $Q = 30$ for the RIS-aided downlink and $Q = 0$ for the RIS-unaided one, respectively. The corresponding analytical curves (7) are plotted by using the parameters (11) and (12) (Approximation 2). Besides corroborating the noticeable accuracy of the proposed approximation, which does not require hardening of the reflection channel, it is seen from Fig. 1 that $\Delta\bar{C}_{\text{sum}}$ decreases with K . This behavior is due to the fact that the increase in K of \bar{C}_{sum} is partially hidden by the larger SNR gain due to reflection process of the RIS, while $\bar{C}_{\text{sum}}^{\text{w/o RIS}}$ scales like $\ln(\ln(K))$.

Fig. 2 and 3 depict the performance of the RIS-aided downlink as a function of the number of meta-atoms Q for different values of ρ , with $K = 10$. In this case, $\bar{C}_{\text{sum}}^{\text{w/o RIS}} = 25.26$ bits/s/Hz. In Fig. 2, the rate \bar{C}_{sum} is compared with the analytical curve (7) by using the parameters (9) (Approximation 1), whereas (11) and (12) (Approximation 2) are used in Fig. 3. Results confirm the precision of Approximation 2 and show that the approximation based on the hardening of the reflection channel (Approximation 1) is inaccurate for small values of Q , especially when the reflection channel is stronger than the direct one. From the comparison among Figs. 1, 2, and 3, it can be inferred that, as predicted, the sum-rate capacity increases much faster with respect to Q than K .

V. CONCLUSIONS

We derived two approximations of the sum-rate capacity of an opportunistic time-sharing downlink with an RIS. The approximation based on the hardening of the reflection channel

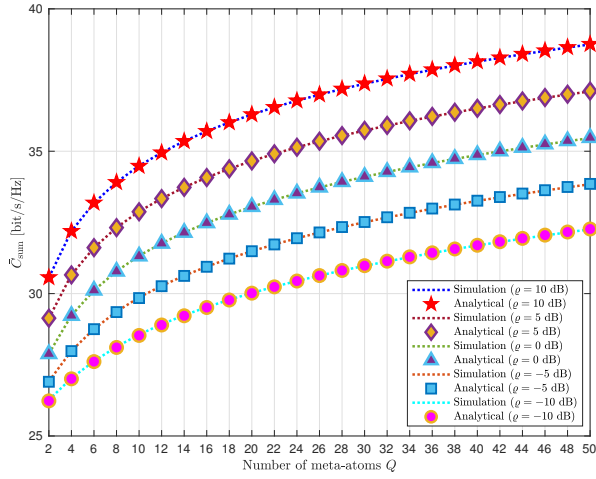


Fig. 3. \bar{C}_{sum} versus Q ($K = 10$, Approximation 2 for the analytical curves).

allows to show the asymptotic scaling laws in terms of the number of users K and the number of meta-atoms Q . A more accurate approximation was derived by approximating the overall channel seen by each user as a gamma RV. Both multiuser diversity and reflection process of the RIS provide increased channel magnitudes. However, the SNR gain increases faster with respect to Q than K and, thus, the multiuser diversity effect becomes negligible even for moderate values of Q . Herein, we have considered single-antenna BS and receivers. An interesting research subject consists of extending the proposed framework to the case of multi-antenna terminals.

APPENDIX A DISTRIBUTIONS OF RVs $Z_k^{(1)}$ AND $Z_k^{(2)}$

The distribution of $Z_k^{(1)}$ does not depend on the number Q of meta-atoms: it is a Rayleigh-distributed RV or, equivalently, it can be seen as a Nakagami RV with shape parameter $m = 1$ and scale parameter $\Omega = \sigma_h^2$ [11]. On the other hand, the distribution of $Z_k^{(2)}$ strongly depends on Q . Indeed, it can be readily verified that $Z_k^{(2)}$ is a Nakagami RV with shape parameter $m = Q$ and scale parameter $\Omega = \sigma_f^2 \sigma_g^2 Q^2$, whose mean and variance are given by (see, e.g., [11])

$$\mathbb{E}[Z_k^{(2)}] = \sigma_f \sigma_g \sqrt{Q} \frac{\Gamma(Q + \frac{1}{2})}{\Gamma(Q)} \approx \sigma_f \sigma_g Q \quad (14)$$

$$\text{VAR}[Z_k^{(2)}] = \sigma_f^2 \sigma_g^2 Q^2 \left\{ 1 - \frac{1}{Q} \left[\frac{\Gamma(Q + \frac{1}{2})}{\Gamma(Q)} \right]^2 \right\} \approx \frac{\sigma_f^2 \sigma_g^2 Q}{4} \quad (15)$$

where $\Gamma(x) \triangleq \int_0^{+\infty} t^{x-1} e^{-t} dt$, with $x > 0$, is the gamma function, whereas the approximations come from the Stirling's series of the quotient $\Gamma(Q + \frac{1}{2})/\Gamma(Q)$ [14] for very large Q .

APPENDIX B CHOICE OF THE PARAMETERS \hat{m} AND $\hat{\Omega}$

To obtain an accurate approximation of $f_{Z_k}(\alpha)$, we resort to the *moment matching* method. Specifically, the parameters \hat{m} and $\hat{\Omega}$ are chosen such that to match the second and fourth

moments of Z_k and \hat{Z}_k , i.e., (i) $\mathbb{E}[Z_k^2] = \mathbb{E}[\hat{Z}_k^2]$ and (ii) $\mathbb{E}[Z_k^4] = \mathbb{E}[\hat{Z}_k^4]$. By observing that $\mathbb{E}[\hat{Z}_k^2] = \mathbb{E}[\hat{X}_k]$, with the mean of the gamma distribution (10) being the ratio between its shape and scale parameters, i.e., $2\hat{m}/(\hat{\Omega}/\hat{m}) = 2\hat{\Omega}$, condition (i) yields $\hat{\Omega} = \frac{\mathbb{E}[Z_k^2]}{2} = \frac{1}{2} \mathbb{E}[X_k]$. Since $\mathbb{E}[\hat{Z}_k^4] = \mathbb{E}[\hat{X}_k^2]$, with the 2-nd moment of the gamma RV \hat{X}_k given [13] by $\mathbb{E}[\hat{X}_k^2] = \left(\frac{\hat{\Omega}}{\hat{m}}\right)^2 \frac{\Gamma(2\hat{m}+2)}{\Gamma(2\hat{m})} = \frac{2\hat{\Omega}^2}{\hat{m}}(2\hat{m}+1)$, where we have also used $\Gamma(x+1) = x\Gamma(x)$, which is in general valid for all complex numbers x except the non-positive integers, condition (ii) leads to $\hat{m} = \frac{1}{2} \frac{\mathbb{E}^2[X_k]}{\mathbb{E}[X_k] - \mathbb{E}^2[X_k]} = \frac{1}{2} \frac{\mathbb{E}^2[X_k]}{\text{VAR}[X_k]}$. By observing that the moments of the Rayleigh RV $|h_k|$ and the chi-distributed RV $\|\mathbf{f}_k\|$ can be expressed as (see, e.g., [11]) $\mathbb{E}[|h_k|^n] = \sigma_h^n \Gamma(1 + \frac{n}{2})$ and $\mathbb{E}[\|\mathbf{f}_k\|^n] = \sigma_f^n \frac{\Gamma(Q + \frac{n}{2})}{\Gamma(Q)}$, for $n \in \mathbb{N}$, it can be shown that the first two moments of X_k are

$$\mathbb{E}[X_k] = \sigma_h^2 + \sigma_f^2 \sigma_g^2 Q^2 + \sigma_f \sigma_g \sigma_h \sqrt{Q} \pi \frac{\Gamma(Q + \frac{1}{2})}{\Gamma(Q)} \quad (16)$$

$$\begin{aligned} \mathbb{E}[X_k^2] &= 2\sigma_h^4 + 3\sigma_f \sigma_g \sigma_h^3 \sqrt{Q} \pi \frac{\Gamma(Q + \frac{1}{2})}{\Gamma(Q)} \\ &\quad + 6\sigma_f^2 \sigma_g^2 \sigma_h^2 Q^2 + 2\sigma_f^3 \sigma_g^3 \sigma_h Q \sqrt{Q} \pi \frac{\Gamma(Q + \frac{3}{2})}{\Gamma(Q)} \\ &\quad + \sigma_f^4 \sigma_g^4 Q^3 (Q + 1) \end{aligned} \quad (17)$$

where $\Gamma(3/2) = \sqrt{\pi}/2$ and $\Gamma(5/2) = 3\sqrt{\pi}/4$ have been used.

REFERENCES

- [1] T.J. Cui, M.Q. Qi, X. Wan, J. Zhao, and Q. Cheng, "Coding metamaterials, digital metamaterials and programmable metamaterials," *Light-Sci. Appl.*, vol. 3, e218, Oct. 2014.
- [2] M. Di Renzo *et al.*, "Smart radio environments empowered by reconfigurable intelligent surfaces: How it works, state of research, and the road ahead," *IEEE J. Select. Areas Commun.*, vol. 38, pp. 2450-2525, Nov. 2020.
- [3] D. Tse and P. Viswanath, *Fundamentals of Wireless Communication*. Cambridge University Press, USA, 2005.
- [4] M. Sharif and B. Hassibi, "A comparison of time-sharing, DPC, and beamforming for MIMO broadcast channels with many users," *IEEE Trans. Commun.*, vol. 55, pp. 11-15, Jan. 2007.
- [5] Q. Wu and R. Zhang, "Intelligent reflecting surface enhanced wireless network via joint active and passive beamforming," *IEEE Trans. Wireless Commun.*, vol. 18, pp. 5394-5409, Nov. 2019.
- [6] M. Di Renzo, F.H. Danufane, and S. Tretyakov, "Communication models for reconfigurable intelligent surfaces: From surface electromagnetics to wireless networks optimization," *Proc. IEEE*, vol. 110, pp. 1164-1209, Sept. 2022.
- [7] M.R. Leadbetter, "Extreme value theory under weak mixing conditions," *Studies in Probab. Theory, MAA Studies in Maths.*, pp. 46-110, 1978.
- [8] E.J. Gumbel, *Statistics of Extremes*. Columbia University Press, 1958.
- [9] S. Kalyani and R.M. Karthik, "The asymptotic distribution of maxima of independent and identically distributed sums of correlated or non-identical gamma random variables and its applications," *IEEE Trans. Commun.*, vol. 60, pp. 2747-2758, Sep. 2012.
- [10] H.Q. Ngo and E.G. Larsson, "No downlink pilots are needed in TDD massive MIMO," *IEEE Trans. Wireless Commun.*, vol. 16, pp. 2921-2935, May 2017.
- [11] J.G. Proakis, *Digital Communications*. New York, NY, USA: McGraw-Hill, 2001.
- [12] Z. Hadzi-Velkov, N. Zlatanov, and G.K. Karagiannidis, "An accurate approximation to the distribution of the sum of equally correlated Nakagami- m envelopes and its application in equal gain diversity receivers," in *Proc. IEEE Int. Conf. Commun. (ICC)*, Dresden, Germany, June 2009, pp. 1-5.
- [13] G. Casella and R.L. Berger, *Statistical Inference*. Pacific Grove, CA: Duxbury/Thompson Learning, 2002.
- [14] G. Arfken, *Stirling's Series (3rd Ed.)*, in *Mathematical Methods for Physicists*, Orlando, FL: Academic Press, pp. 555-559, 1985.